Optimal Structure and Size of Multi-segment Soft Robotic Arms with Finite Element Method

Xiaohui Li[1, 2], Wei Zhang[1], and Liping Zhao[1, *]

[1] Technology and Engineering Center for Space Utilization, Chinese Academy of Sciences, Beijing, China
[2] University of Chinese Academy of Sciences, Beijing, China

Abstract. Pneumatic actuate of multi-segment soft robotic arm is a significant structure and has extensive applications. However, the study of the optimal structure and size of multi-segment soft robotic arm has not been achieved. In this study, the finite element method is used to optimized the structure and size of soft robotic arm. We report that the two-segment structure of soft robotic arm has better performance for the general manipulator operation task through evaluating bending angles with different structures and parameters. The optimal ratio of the total length of non-cavity section to the total length of the soft robotic arm with two-segment is 0.21. And soft robotic arm performs better when the length of the fixed first section, the linkage section between two cavity sections and the end section are equal. Two cavities in each segment has more advantages in tasks of plane bending, while three cavities structure has better adaptability when the task need bend in the space. These results in this study provide a reference and simplify the process for the structure and size design of the multi-segment soft robotic arm in the future.

1 Introduction

The soft robotic arm is inspired by creatures including elephant trunk and octopus tentacles [1-2]. Soft robotic arms are characterized by low stiffness, high compliant, multiple degrees of freedom [3-5] and improved safety in human interaction compared with rigid mechanical arms. It has extensive applications in various fields [6, 7]. Pneumatic actuate of soft robotic arms is a common structure in design which can produce large deformation of bending and simply to control and achieve.

Pneumatic actuate of soft robotic arm has various structure [8-11]. One single-cavity structure can bend to a fixed direction after the cavity is filled with certain air pressure and only suit for the task requirements of bending in fixed direction [12, 13], such as wearable gloves [14-16]. For meeting more work requirements and accomplishing bend in multiple directions, two-cavity structure [17] and three-cavity structure [18-20] of soft robotic arms appeared. Soft robotic arms with these structures can bend in different directions by controlling pressure to one or more cavities to produce the desired bending effect. Yahya Elsayed [21] optimized the structure and cavity size with the finite element method for three-cavity soft robotic arms, but this was only the design optimized for single-segment robotic arms. The appearance of a soft robotic arm with multi-segments further expand the application scenarios of soft robotic arms and meet more complex working requirements [22, 23]. Each segment also has multiple cavities, which can bend in different directions. A soft robotic arm with this structure can achieve complex bending shapes including hook-shaped bending and S-shaped bending by controlling pressurizing of different segments and cavities [24]. The radial expansion was limited and the deformation was mainly reflected in the axial direction through wrapping the fiber on the outer surface of the soft robotic arm [25].

Modelling of soft robotic arms have always been a tough problem and there has been no accurate method. Most of researches simplified modelling process with the assumption of piecewise constant curvature [9] and accomplished modelling process using the coordinate transformation method of rigid mechanical arms [26]. There are inevitable errors in this modelling method. Furthermore, the specific way and results of modelling are different for various structures and sizes of soft robotic arms. Thus, there is no unified approach to modelling soft robotic arms. The optimal structure and size of soft robotic arms cannot be obtained by theoretical analysis because of these problems. A new method is desired to optimize the design process of soft robotic arms. The design method of finite element analysis has been applied in various fields. This method can handle the problem of complicated situations and optimize design stage. This method is more convenient and advantageous.

In this study we first optimize the number of segments of soft robotic arms based on multi-cavity and multi-segment structure by finite element analysis. Moreover, we continue optimize the ratio of the total length of non-cavity section to the total length of the soft robotic arm, the length of the linkage section between cavity sections, and the length of the fixed first and end section. Finally,

* Corresponding author: zhaoliping@csu.ac.cn

we compare the performance of the two-cavity and three cavity structure of soft robotic arm.

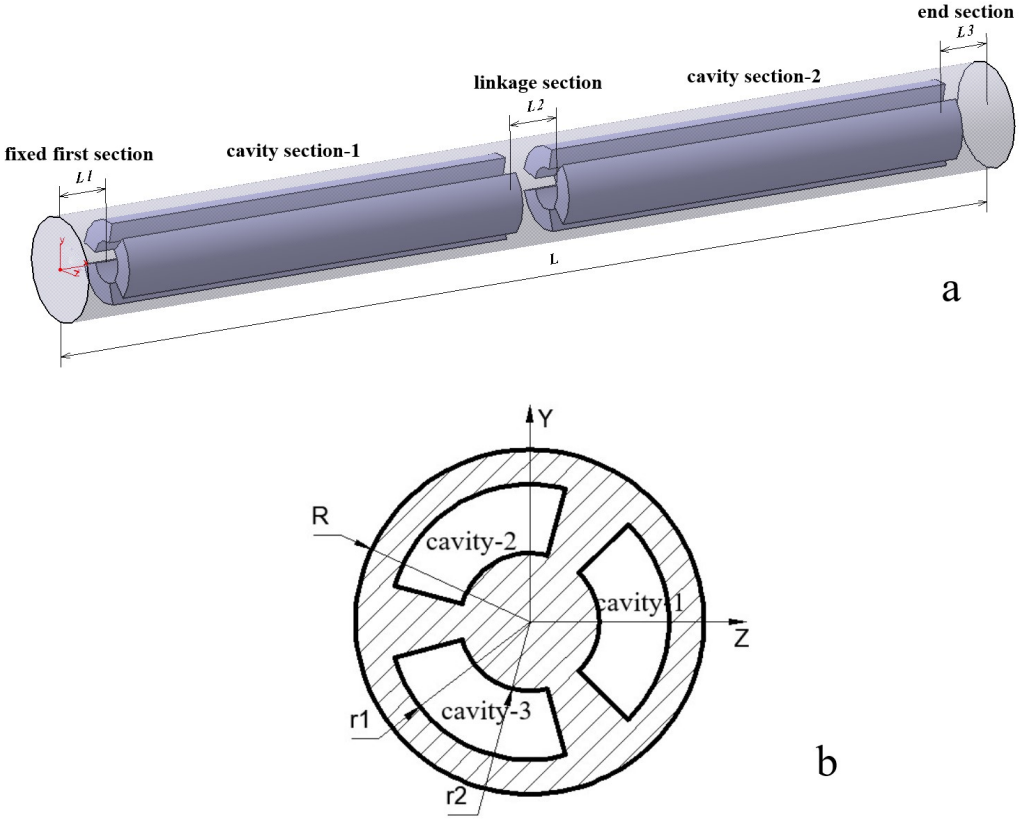

Figure 1. Schematic diagram of soft robotic arm with three cavities in each segment. (a) two-segment structure soft robotic arm including fixed first section, linkage section, end section and two cavity sections. (b) the cross section of soft robotic arm with three cavities.

2 Materials and Methods

2.1 Design of soft robotic arm

The soft robotic arm was designed as three types including two-segment, three-segment, and four-segment structure. The total length was L consisted of the fixed first section with length L_1, the linkage section (one or more, a single length L_2) between two cavity sections, and the end section (L_3) were shown in Figure 1. The structure with three cavities in a cavity section was optimized for design. According to the results of [17], the radius of soft robotic arm was $R = 10mm$, and the radius of the sector cavity was $r_1 = 8mm$ and r_2=$4mm$ respectively. The angle of each sector was 90°, so the interval between each sector was 30°. The origin of coordinates was defined as the center of the fixed first section circle. The axis along the soft robotic arm was X axis, the right was Z axis, and the upward was Y axis.

2.2 Finite element method

The following three processes were included by the design of finite element method.

Firstly, the CATPart format model in CATIA was imported into ABAQUS and the material property was set as superelastomer. Two radial constraint rope Parts were established in ABAQUS, one was clockwise winding and another was anticlockwise winding. The material property was rigid. The three Parts were assembled and the interaction between the two radial constraint ropes and the soft robotic arm were set as embedding. The direction of gravity was positive along the Z axis, and the magnitude of gravitational acceleration is $9.8m/s^2$. The soft robotic arm can produce an arc-shaped bending by pressuring cavitiy-1 of each segment.

Secondly, the bending angle (0~180°) of the end section plane to the fixed first section plane, that is, the coordinate plane YZ was measured.

Thirdly, the design parameters were changed, and a series of bending angles were obtained. The optimal value was to maximize the bending angle.

2.3 Parameters and materials properties

The parameters to be optimized included the number of segments (two segments, three segments and four segments), the ratio of the total length of non-cavity section to the total length of the soft robotic arm, defined as $ratio1 = \frac{L_1 + L_2 + L_3}{L}$, the length of the linkage section between cavity sections, and the length of the fixed first and end section.

The material of the soft robotic arm was Elastomer M4601 (Wacker Inc.) with a density of $1.2g/cm^3$ [19]. Yeoh second-order model of the superelastomer constitutive model was adopted and material was isotropic with the model function of

$$w_i = C_{10}(I_1 - 3)^1 + C_{20}(I_1 - 3)^2. \quad (1)$$

The strain invariant C_{10}=0.11Mpa, $C_{20} = 0.02Mpa$. The radial winding ropes was made of polyethylene with a density of $7.83g/cm^3$, Young's modulus of 31067Mpa, and Poisson's ratio of 0.36[19].

The actuators were meshed in C3D8R elements and the element of the polyethylene was set to be T3D2. The elements number of two-segment soft robotic arm was 731 and the number of nodes was 1104, while the three-segment was 1078 and 1584 and four-segment was 743 and 1080.The elements number of radial constraint rope was always 242.

3 Results

The sort robotic arm occurred axial elongation and radial expansion when the cavity was pressurized. Wingding the rigid constraint rope limited radial expansion so that the main deformation was in the axial direction [27, 28]. Then the soft robotic arm generated bending. Nine points were selected on the end surface after deformation, including a centre point, four inner circle points and four outer circle points as shown in Figure 2. The end surface plane was fitted by these nine points and the relative position of the end surface in the coordinate system of the fixed plane was determined. A series of bending angle values were obtained after changing the parameters that to be optimized. Compared the angles values to obtained the optimal parameters. The simulation time was set 1s.

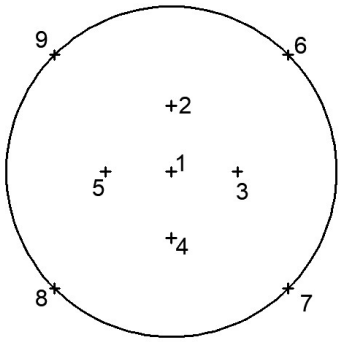

Figure 2. Schematic diagram of nine points on the end surface.

3.1 Optimize the number of segments

The soft robotic arm was designed into two-segment, three-segment and four-segment structure. Each cavity section consisted of three cavities. The total length of soft robotic arm was same, L=200mm. The ratio1 varied from 0.06 to 0.24 with an interval of 0.03. Two-segment, three-segment and four-segment structure contained three, four and five non-cavity sections respectively and the length of each non-cavity section was equal. The soft robotic arm can produce an arc-shaped bending by pressuring cavities with 0.1Mpa and 0.2Mpa at same location of each segment. The bending angles were obtained through measured the position of the end section surface in the coordinate system. A series of angle values were drawn in Figure 3. When the pressure was 0.1Mpa, the soft robotic arm with four-segment structure cannot bending resisting gravity, the "four-segment, 0.1Mpa" was missed in the Figure3.

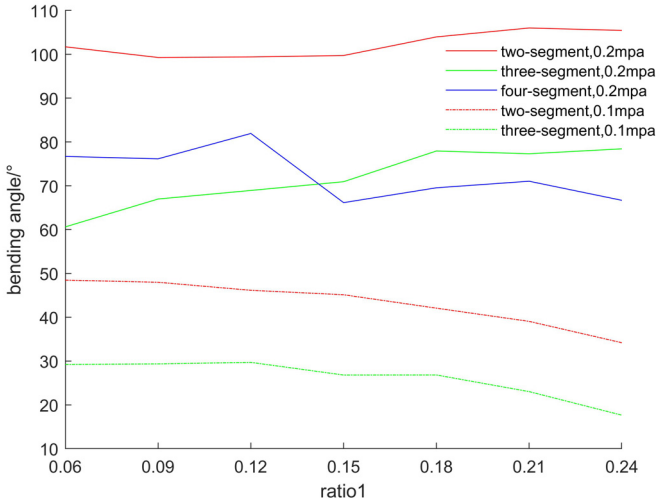

Figure 3. The bending angles of multi-segment soft robotic arm with different ratio1 under 0.1Mpa and 0.2Mpa. Ratio1 is the total length of non-cavity section to the total length of the soft robotic arm (200mm).

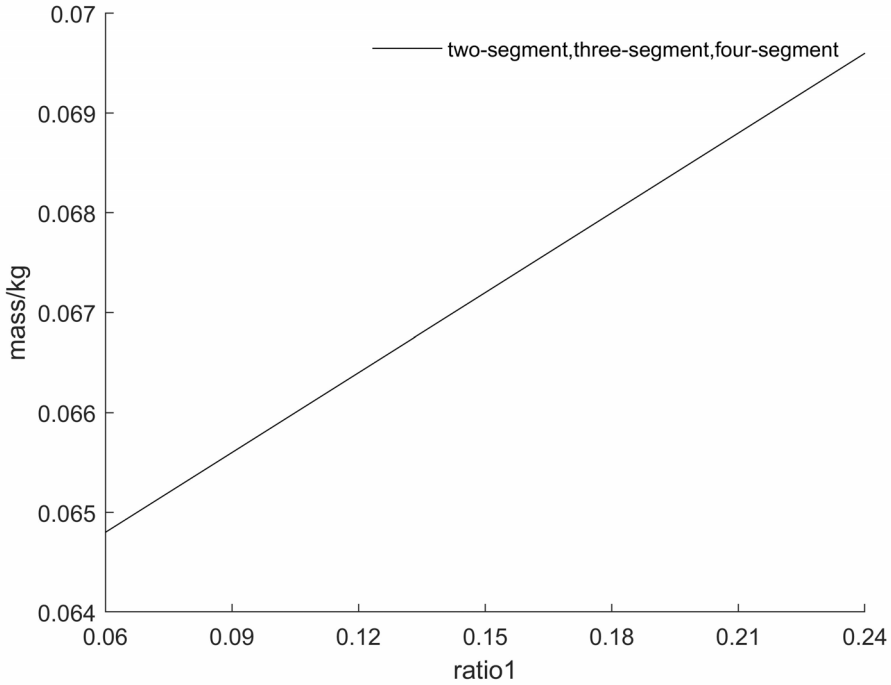

Figure 4. The mass of soft robotic arm under different ratio1. The two-segment, three-segment and four-segment structure of soft robotic had same mass under the same ratio1.

The soft robotic arm with two-segment structure performed lager bending angle than three-segment and four-segment structure regardless of 0.1Mpa and 0.2Mpa. The mass of soft robotic arm linearly increased with the ratio1 increased as shown in Figure 4. Figure 3 shown when pressure was 0.1Mpa, the bending angle decreased with the increase of ratio1 because of the increasing mass. When pressure was 0.2Mpa, the bending angle of two-segment and three-segment structure increased with the ratio1 increased. The comparison of these two results shows that the two-segment and three-segment structure of soft robotic arm performed better under high pressure.

The two-segment structure of soft robotic arm can produce arc-shaped bending, hook-shaped bending, and S-shaped bending [12], which was enough for requirements of most tasks. The two-segment soft arm needs to control six cavities, while the three-segment and four-segment structure need control nine and twelve cavities, respectively. More cavities are more difficult for manufacturing and control system. Therefore, the two-segment structure is sufficient for the general manipulator operation task. The three-segment and four-segment structure of soft robotic arm would suit for specific task. The two-segment structure of soft robotic arm is optimized in following part.

3. 2 Optimize the total length of non-cavity section

The optimal total length of non-cavity section varied with different total length of soft robotic arm. Hence, the ratio of the total length of non-cavity section to the total length of the soft robotic arm was chosen as the objective of design, that is ratio1. And the length of each non-cavity section was designed equal.

The two-segment structure of soft robotic arm with more extensive application was selected and the total length soft arm, L, was changed to 300mm. The ratio1 varied from 0.06 to 0.24 with an interval of 0.03. The bending angles under pressure of 0.1Mpa and 0.2Mpa were measured. Figure 5(a) presented the bending angles at different ratios when the total length of the soft robotic arm was 200mm and 300mm. The soft robotic arm of 300mm under 0.1Mpa also cannot bend resisting gravity. Hence, the “L=300mm, 0.1mpa" was missed.

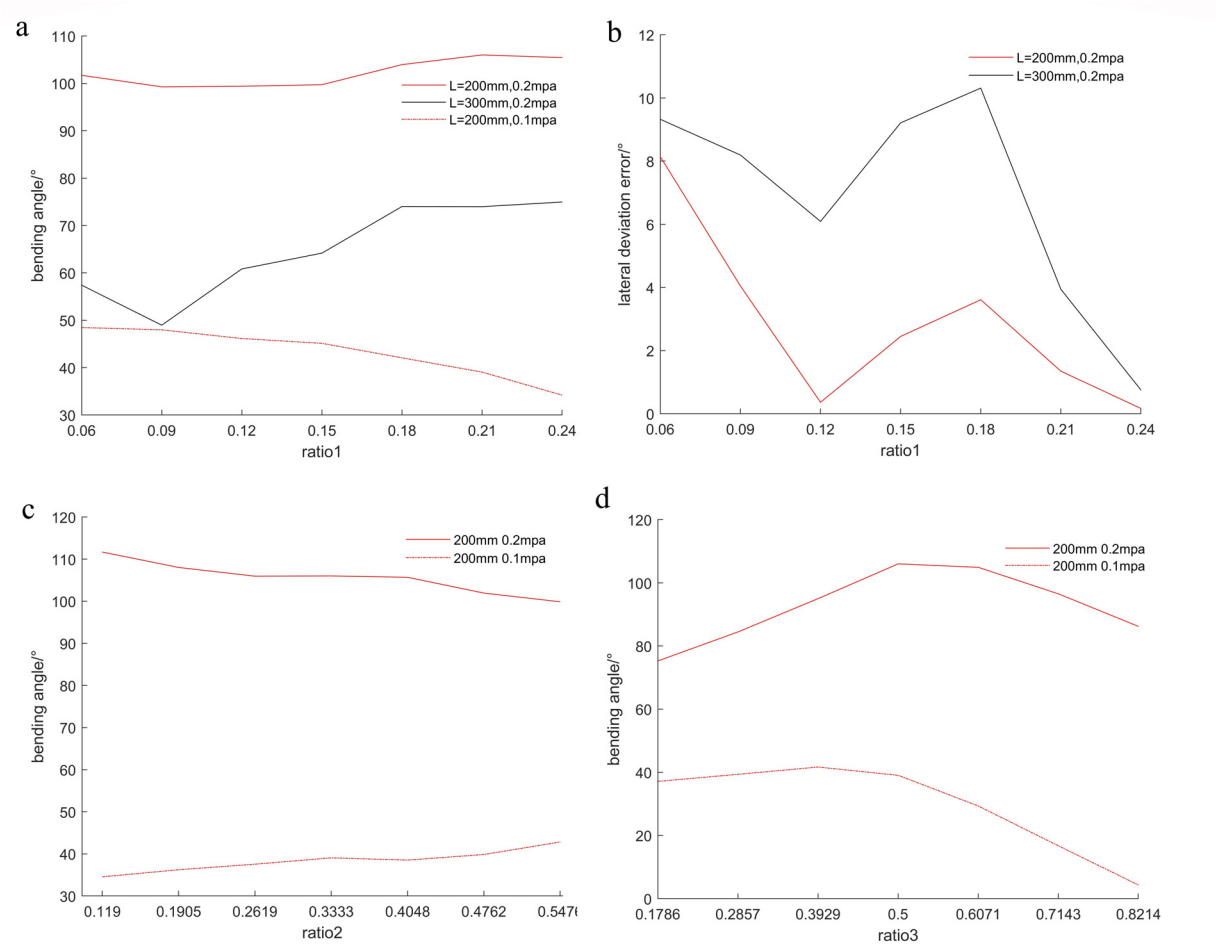

Figure 5. (a) The bending angles at different ratios when the total length of the soft robotic arm was 200mm. Ratio1 is the total length of non-cavity section to the total length of the soft robotic arm. (b) The lateral deviation error of 200mm soft robotic arms under pressure conditions of 0.1Mpa and 0.2Mpa. (c) The tuning of the length of linkage section under 0.1Mpa and 0.2Mpa. Ratio2 is the length of linkage section to the total length of non-cavity section. (d) The tuning of the length of fixed first section under 0.1Mpa and 0.2Mpa. Ratio3 is the length of the fixed first section to the sum length of the fixed first section and the end section.

When the pressure was 0.1Mpa, the bending angle decreased with the increase of ratio1 because of the increasing mass. When the pressure was 0.2Mpa, the bending angle was larger under ratio1 was 0.18, 0.21 and 0.24. The soft robotic arm with total length 200mm performance better than 300mm because the mass would significantly increase with the total length increase.

Figure 5(b) presented the lateral deviation error of 200mm and 300mm soft robotic arms under pressure conditions of 0.2Mpa. The lateral deviation error was the difference between the angle between the end surface and XZ and 90 degrees. It was obvious that the deviation error of the 200mm soft robotic arm less than that of the 300mm soft robotic arm. Therefore, the deviation error should be considered when designing the longer two-segment soft robotic arm.

The bending performance, the lateral deviation error and the mass of soft robotic arm were taken into account, the optimal ratio1 was chosen 0.21. And the total length of soft robotic arm was chosen 200mm in following parts. Therefore, the total length of non-cavity section was 42mm.

3. 3 Optimize the length of linkage section

The total length of non-cavity section was 42mm when the length of the two-segment soft robotic arm was 200mm and the ratio1 was 0.21. The ratio of the length of linkage section to the total length of non-cavity section, defined as $ratio2 = \frac{L_2}{L_1 + L_2 + L_3}$, varied according to 0.1190, 0.1905, 0.2619, 0.3333, 0.4048, 0.4762, 0.5476 and the length of the fixed first section and the end section was equal. The bending angles of two-segment soft robotic arm were measured under 0.1Mpa and 0.2Mpa.

Figure 5(c) presented that when the pressure was 0.1Mpa, the bending angle increased with the ratio2 increased and when the pressure was 0.2Mpa, the bending angle decreased with the ratio2 increased. The soft robotic arm should have better working performance under high pressure(0.2Mpa) and low pressure(0.1Mpa), the optimal ratio2 was chosen 0.3333. The length of linkage section was 14mm.

3.4 Optimize the length of fixed first section

The length of two-segment soft robotic arm was 200mm. The ratio1 was 0.21and the ratio2 was 0.3333. Therefore, the sum of the length of the fixed first section and the end section was 28mm. The ratio of the length of the fixed first section to the sum length of the fixed first section and the end section, defined as $ratio3 = \frac{L_1}{L_1 + L_3}$, varied according 0.1786, 0.2857, 0.3929, 0.5000, 0.6071, 0.7143, 0.8214. The bending angles of two-segment soft robotic arm were measured under 0.1Mpa and 0.2Mpa.

Figure 5(d) presented the variation trend of bending angle was increase first and then decrease with the increase of the ratio3. The angle of soft robotic arm was largest when the ratio3 was 0.5000. At this ratio, the length of the fixed first section of 200mm soft robotic arm was 14mm.

3. 5 Optimize selection of cavity structure

Each segment included two cavities or three cavities. Two cavities soft robotic arm can only bend in the plane, while three cavities can bend in space. The two-segment soft robotic arm of two different number of cavities generated S-shaped bending under pressure conditions of 0.1Mpa and 0.15Mpa as shown in Figure 6. Each cavity of the two structures were of equal volume. Red was the two cavities structure, in which the opposite cavity of two segments were pressurized. Blue was the three cavities structure, in which one cavity of a segment and two cavities of another segment were pressurized.

Figure 6 presented the effect and angle of bending of two cavities structure soft robotic arm were better than three cavities under the same pressure. Therefore, the two cavities structure had greater advantages and was relatively simple to actuate and control when the task can be completed only by plane bending. The three cavities structure had better adaptability when the task need bend in the space.

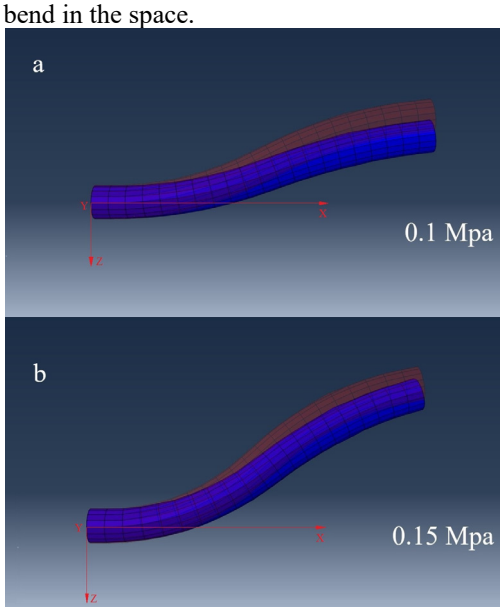

Figure 6. The effect and angle of bending of soft robotic arm under 0.1Mpa and 0.15Mpa. Red is the two cavities structure and blue are the three cavities structure.

4 Discussion

In this study, the structure and size of multi-segment soft robotic arm are optimized with finite element analysis. The position of end plane was fitted by nine points which were selected on the end surface after deformation. The relative position of the end surface in the coordinate system of the fixed plane was determined and then the bending angles were obtained. The soft robotic arm can produce an arc-shaped bending by pressuring cavitiy-1 of each segment. The performance of the soft robotic arm was evaluated by comparing the bending angles.

The two-segment structure of soft robotic arm with the total length of 200mm performances 39.0539°, 106.0135° of bending angle respectively under 0.1Mpa and 0.2Mpa pressurized when each section is optimal as shown in Figure 7. The optimal size is the length of the fixed first section, the linkage section between two cavity sections and the end section equal to 14mm. Under this condition, the maximum mises stress of soft robotic arm is 0.5918Mpa and the maximum principal strain is 0.5004mm. The result is far less than the tensile strength of the material.

The soft robotic arm with the total length of 200mm in [24] produce 47.2052°, 97.9023° respectively under 0.1Mpa and 0.2Mpa pressurized. The mass of soft robotic arm in [24] is 65. 8g while the mass in this paper with the optimal structure is 68.8g. The soft robotic arm performance of this paper results is significantly better under high pressure (0.2Mpa).

Soft materials are characterized by low stiffness and light weight and soft robotic arms have multiple degrees of freedom of movement and high compliance. So soft robotic arms are generally used in special environment in which rigid manipulator not suitable, such as unknown environment exploration, medical diagnosis and treatment. In these application scenarios, the low load is bear for soft robotic arm. When the load is 0.4N (center point of the end surface, along Z axis) and the pressure is 0.3Mpa, the bending angle generated by the soft robotic arm in reference [20] is 93.2645°, less than 111.2430° generated by the soft robotic arm in my manuscript. Therefore, the results of this paper have meaningfully importance for maximizing the performance of the soft robotic arm.

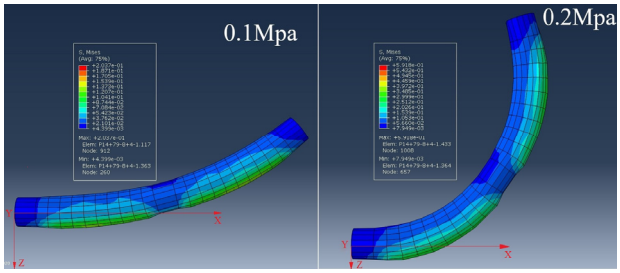

Figure 7. The deformation of the soft robotic arm with optimal structure under 0.1Mpa and 0.2Mpa.

5 Conclusions

We draw conclusions through simulating in ABAQUS and comparing the bending angles. The two-segment structure of soft robotic arm has better performance than

three-segment and four-segment structure for the general manipulator operation task. The optimal ratio of the total length of non-cavity section to the total length of the soft robotic arm with two-segment is 0.21. The two-segment soft robotic arm performs better when the length of the fixed first section, the linkage section between two cavity sections and the end section are equal. The soft robotic arm with two cavities in each segment has more advantages in tasks of plane bending, while three cavities structure has better adaptability when the task need bend in the space. This study presents the design method in dimension of each section for multi-segment soft robotic arm. These conclusions in this study provides a reference for the structure and size design of the multi-segment soft robotic arm, so that the soft robotic arm can produce better performance to the requirements of complex tasks. The optimal structure of soft robotic arm can be chosen in different conditions of working environment.

The deviation error was showed as in the angle between the end surface and XZ plane. In future work, the error can also be showed as displacement in Y or several ways together to express error. And the variation of deviation error can be researched with different parameters and structure of soft robotic arm. The deviation error should be considered in evaluating the bending performance in the future.

References

1. L. Margheri, C. Laschi, B. Mazzolai. Soft robotic arm inspired by the octopus: I. From biological functions to artificial requirements. Bioinspiration & Biomimetics, 2012, 7(2):025004.
2. M. Sfakiotakis, A. Kazakidi, D. P. Tsakiris. Octopus-inspired multi-arm robotic swimming. Bioinspiration & Biomimetics, 2015, 10(3):035005.
3. L. Wang, SG. Nurzaman, F. Iida. Soft-Material Robotics. Foundations & Trends in Robotics, 2014; 5(3):1-75.
4. F. Schmitt, O. Piccin, L. Barbe, et al. Soft Robots Manufacturing: A Review. Frontiers in Robotics and AI 2018; 5:84.
5. K. Chubb, D. Berry, T. Burke. Towards an ontology for soft robots: What is soft?. Bioinspiration & Biomimetics, 2019, 14(6).
6. Amendjohn, Chengnadia, Fakhourisami, et al. Soft Robotics Commercialization: Jamming Grippers from Research to Product. Soft robotics 2016;3(4): 213-222.
7. D. Rus, MT. Tolley. Design, fabrication and control of soft robots. Nature 2015; 521(7553): 467-475.
8. Y. Hao, Z. Gong, Z. Xie, et al. Universal soft pneumatic robotic gripper with variable effective length. Chinese control conference 2016: 6109-6114.
9. G. Singh, G. Krishnan. Designing Fiber-Reinforced Soft Actuators for Planar Curvilinear Shape Matching. Soft robotics 2020;7(1): 109-121.
10. KC. Galloway, Y. Chen, E. Templeton, et al. Fiber Optic Shape Sensing for Soft Robotics. Soft robotics 2019; 6(5): 671-684.
11. Y. Zhang, N. Zhang, H. Hingorani, et al. Fast - Response, Stiffness - Tunable Soft Actuator by Hybrid Multimaterial 3D Printing. Advanced Functional Materials 2019; 29(15).
12. KC. Galloway, KP. Becker, B. Phillips, et al. Soft Robotic Grippers for Biological Sampling on Deep Reefs. Soft robotics 2016; 3(1): 23-33.
13. Z. Wolf, A. Jusufi, D. Vogt, et al. Fish-like aquatic propulsion studied using a pneumatically-actuated soft-robotic model. Bioinspiration & Biomimetics, 2020, 15(4).
14. L. Ge, F. Chen, D. Wang, et al. Design, Modeling, and Evaluation of Fabric-Based Pneumatic Actuators for Soft Wearable Assistive Gloves. Soft robotics 2020;
15. P. Polygerinos, Z. Wang, KC. Galloway, et al. Soft robotic glove for combined assistance and at-home rehabilitation. Robotics and Autonomous Systems 2015; 135-143.
16. G. Agarwal, N. Besuchet, B. Audergon, et al. Stretchable Materials for Robust Soft Actuators towards Assistive Wearable Devices. Scientific Reports 2016; 6(34224): 34224-34224.
17. G. Gerboni, A. Diodato, G. Ciuti, et al, Menciassi A. Feedback Control of Soft Robot Actuators via Commercial Flex Bend Sensors. IEEE-ASME Transactions on Mechatronics 2017; 22(4): 1881-1888.
18. SM. Mustaza, Y. Elsayed, C. Lekakou, et al. Dynamic modeling of fiber-reinforced soft manipulator: A visco-hyperelastic material-based continuum mechanics approach. Soft robotics 2019; 6(3): 305-317.
19. X. Peng, N. Zhang, L. Ge, et al. Dimension Optimization of Pneumatically Actuated Soft Continuum Manipulators. 2019 2nd IEEE International Conference on Soft Robotics (RoboSoft), Seoul, Korea (South) 2019; 14-18.
20. A. D. Marchese, R. Daniela. Design, kinematics, and control of a soft spatial fluidic elastomer manipulator. The International Journal of Robotics Research. 2016;35(7):840-869.
21. Y. Elsayed, A. Vincensi, C. Lekakou, et al. Finite Element Analysis and Design Optimization of a Pneumatically Actuating Silicone Module for Robotic Surgery Applications. Soft robotics 2014; 1(4): 255-262.
22. RK. Katzschmann, CD. Santina, Y. Toshimitsu, et al. Dynamic Motion Control of Multi-Segment Soft Robots Using Piecewise Constant Curvature Matched with an Augmented Rigid Body Model. Robosoft19. 2019.
23. F. Giorgio-Serchi, A. Arienti, F. Corucci, et al. Hybrid parameter identification of a multi-modal

underwater soft robot. Bioinspiration & Biomimetics, 2017, 12(2):025007.

24. X. Li, L. Zhao, W. Zhang. Hook-Shaped Bending and S-Shaped Bending of Soft Robotic Arm. 2020 4th International Conference on Robotics and Automation Sciences (ICRAS) 2020;1-5
25. G. Singh, C. Xiao, ET. Hsiao-Wecksler, et al. Design and analysis of coiled fiber reinforced soft pneumatic actuator. Bioinspiration & Biomimetics, 2018.
26. S. Grazioso, GD. Gironimo, B. Siciliano. A Geometrically Exact Model for Soft Continuum Robots: The Finite Element Deformation Space Formulation. Soft robotics 2019; 6(6): 790-811.
27. G. Singh, G. Krishnan. A constrained maximization formulation to analyze deformation of fiber reinforced elastomeric actuators. Smart Materials and Structures 2017; 26(6).
28. F. Connolly, CJ. Walsh, K. Bertoldi. Automatic design of fiber-reinforced soft actuators for trajectory matching. Proceedings of the National Academy of Sciences of the United States of America 2017; 114(1): 51-56.